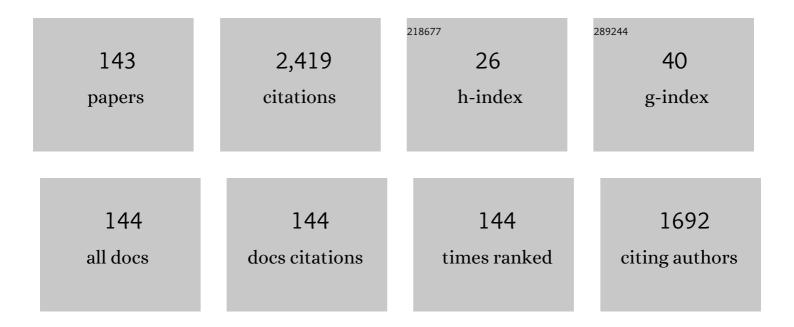
List of Publications by Year in descending order

Source: https://exaly.com/author-pdf/8782005/publications.pdf Version: 2024-02-01



#	Article	IF	CITATIONS
1	Climatology of the planetary boundary layer over the continental United States and Europe. Journal of Geophysical Research, 2012, 117, .	3.3	297
2	Investigation of near-global daytime boundary layer height using high-resolution radiosondes: first results and comparison with ERA5, MERRA-2, JRA-55, and NCEP-2 reanalyses. Atmospheric Chemistry and Physics, 2021, 21, 17079-17097.	4.9	99
3	Trends in Planetary Boundary Layer Height over Europe. Journal of Climate, 2013, 26, 10071-10076.	3.2	86
4	Latitudinal and seasonal variations of inertial gravity wave activity in the lower atmosphere over central China. Journal of Geophysical Research, 2007, 112, .	3.3	58
5	A statistical study of gravity waves from radiosonde observations at Wuhan (30° N, 114° E) China. Annales Geophysicae, 2005, 23, 665-673.	1.6	55
6	Self-Template Synthesis of Ag–Pt Hollow Nanospheres as Electrocatalyst for Methanol Oxidation Reaction. Langmuir, 2017, 33, 5991-5997.	3.5	44
7	A numerical study of propagation characteristics of gravity wave packets propagating in a dissipative atmosphere. Journal of Geophysical Research, 2002, 107, ACL 14-1.	3.3	43
8	Climatology of the diurnal tides from eCMAM30 (1979 to 2010) and its comparison with SABER. Earth, Planets and Space, 2014, 66, 103.	2.5	41
9	Numerical simulation of the 6 day wave effects on the ionosphere: Dynamo modulation. Journal of Geophysical Research: Space Physics, 2016, 121, 10,103.	2.4	41
10	Global climatological variability of quasi-two-day waves revealed by TIMED/SABER observations. Annales Geophysicae, 2013, 31, 1061-1075.	1.6	38
11	Nonlinear coupling between quasi 2 day wave and tides based on meteor radar observations at Maui. Journal of Geophysical Research D: Atmospheres, 2013, 118, 10,936.	3.3	36
12	Formation and Evolution of Low‣atitude <i>F</i> Region Fieldâ€Aligned Irregularities During the 7–8 September 2017 Storm: Hainan Coherent Scatter Phased Array Radar and Digisonde Observations. Space Weather, 2018, 16, 648-659.	3.7	35
13	High vertical resolution analyses of gravity waves and turbulence at a midlatitude station. Journal of Geophysical Research, 2012, 117, .	3.3	34
14	Midlatitude ionospheric responses to the 2013 SSW under high solar activity. Journal of Geophysical Research: Space Physics, 2016, 121, 790-803.	2.4	34
15	Responses of Quasi 2ÂDay Waves in the MLT Region to the 2013 SSW Revealed by a Meteor Radar Chain. Geophysical Research Letters, 2017, 44, 9142-9150.	4.0	34
16	Simultaneous observations of sporadic Fe and Na layers by two closely colocated resonance fluorescence lidars at Wuhan (30.5°N, 114.4°E), China. Journal of Geophysical Research, 2007, 112, .	3.3	33
17	Seasonal variations of the nocturnal mesospheric Na and Fe layers at 30°N. Journal of Geophysical Research, 2009, 114, .	3.3	33
18	TIMED/SABER observations of lower mesospheric inversion layers at low and middle latitudes. Journal of Geophysical Research, 2012, 117, .	3.3	33

#	Article	IF	CITATIONS
19	Latitudinal and altitudinal variability of lower atmospheric inertial gravity waves revealed by U.S. radiosonde data. Journal of Geophysical Research D: Atmospheres, 2013, 118, 7750-7764.	3.3	33
20	Lidar observations of sporadic Na layers over Wuhan (30.5°N, 114.4°E). Geophysical Research Letters, 2002, 29, 59-1-59-4.	4.0	32
21	Observations of thermosphere and ionosphere changes due to the dissipative 6.5-day wave in the lower thermosphere. Annales Geophysicae, 2015, 33, 913-922.	1.6	32
22	Latitudinal and seasonal variations of lower atmospheric inertial gravity wave energy revealed by US radiosonde data. Annales Geophysicae, 2010, 28, 1065-1074.	1.6	30
23	Study of the Quasiâ€5â€Ðay Wave in the MLT Region by a Meteor Radar Chain. Journal of Geophysical Research D: Atmospheres, 2018, 123, 9474-9487.	3.3	30
24	A numerical study of nonlinear propagation of a gravity-wave packet in compressible atmosphere. Journal of Geophysical Research, 1999, 104, 14261-14270.	3.3	27
25	A nonlinear interaction event between a 16-day wave and a diurnal tide from meteor radar observations. Annales Geophysicae, 2013, 31, 2039-2048.	1.6	27
26	Atmospheric tides in the lowâ€latitude <i>E</i> and <i>F</i> regions and their responses to a sudden stratospheric warming event in January 2010. Journal of Geophysical Research: Space Physics, 2013, 118, 7913-7927.	2.4	27
27	Midnight ionosphere collapse at Arecibo and its relationship to the neutral wind, electric field, and ambipolar diffusion. Journal of Geophysical Research, 2012, 117, .	3.3	26
28	Selfâ€Acceleration and Instability of Gravity Wave Packets: 2. Twoâ€Dimensional Packet Propagation, Instability Dynamics, and Transient Flow Responses. Journal of Geophysical Research D: Atmospheres, 2020, 125, e2019JD030691.	3.3	26
29	Nonlinear interaction of gravity waves in a nonisothermal and dissipative atmosphere. Annales Geophysicae, 2014, 32, 263-275.	1.6	23
30	Temperature responses to the 11 year solar cycle in the mesosphere from the 31 year (1979–2010) extended Canadian Middle Atmosphere Model simulations and a comparison with the 14 year (2002–2015) TIMED/SABER observations. Journal of Geophysical Research: Space Physics, 2017, 122, 4801-4818.	2.4	23
31	Gravity wave excitation through resonant interaction in a compressible atmosphere. Geophysical Research Letters, 2009, 36, .	4.0	22
32	Lowâ€latitude daytime <i>F</i> region irregularities observed in two geomagnetically quiet days by the Hainan coherent scatter phased array radar (HCOPAR). Journal of Geophysical Research: Space Physics, 2017, 122, 2645-2654.	2.4	22
33	Hainan Coherent Scatter Phased Array Radar (HCOPAR): System Design and Ionospheric Irregularity Observations. IEEE Transactions on Geoscience and Remote Sensing, 2017, 55, 4757-4765.	6.3	21
34	MF radar observation of mean wind and tides of winter mesopause (80–) region over Wuhan (30°N,) Tj ETQq	0 0 0 rgBT	Qyerlock]
35	Reflection and transmission of atmospheric gravity waves in a stably sheared horizontal wind field. Journal of Geophysical Research, 2010, 115, .	3.3	20

#	Article	IF	CITATIONS
37	Quasi 10―and 16â€Day Wave Activities Observed Through Meteor Radar and MST Radar During Stratospheric Final Warming in 2015 Spring. Journal of Geophysical Research D: Atmospheres, 2019, 124, 6040-6056.	3.3	20
38	Simultaneous and common-volume three-lidar observations of sporadic metal layers in the mesopause region. Journal of Atmospheric and Solar-Terrestrial Physics, 2013, 102, 172-184.	1.6	19
39	A Study on the Quarterdiurnal Tide in the Thermosphere at Arecibo During the February 2016 Sudden Stratospheric Warming Event. Geophysical Research Letters, 2018, 45, 13,142.	4.0	19
40	Latitudinal and Topographical Variabilities of Free Atmospheric Turbulence From Highâ€Resolution Radiosonde Data Sets. Journal of Geophysical Research D: Atmospheres, 2019, 124, 4283-4298.	3.3	19
41	A numerical study on the propagation and evolution of resonant interacting gravity waves. Journal of Geophysical Research, 2004, 109, .	3.3	18
42	Diurnal variations of the planetary boundary layer height estimated from intensive radiosonde observations over Yichang, China. Science China Technological Sciences, 2014, 57, 2172-2176.	4.0	18
43	The interaction between the tropopause inversion layer and the inertial gravity wave activities revealed by radiosonde observations at a midlatitude station. Journal of Geophysical Research D: Atmospheres, 2015, 120, 8099-8111.	3.3	18
44	A Statistical Analysis of the Propagating Quasi 16â€Day Waves at High Latitudes and Their Response to Sudden Stratospheric Warmings From 2005 to 2018. Journal of Geophysical Research D: Atmospheres, 2019, 124, 12617-12630.	3.3	18
45	Intensive radiosonde observations of the diurnal tide and planetary waves in the lower atmosphere over Yichang (111°18' E, 30°42' N), China. Annales Geophysicae, 2009, 27, 1079-1095.	1.6	17
46	Intensive radiosonde observations of lower tropospheric inversion layers over Yichang, China. Journal of Atmospheric and Solar-Terrestrial Physics, 2009, 71, 180-190.	1.6	17
47	Spatial and seasonal variability of medium- and high-frequency gravity waves in the lower atmosphere revealed by US radiosonde data. Annales Geophysicae, 2014, 32, 1129-1143.	1.6	16
48	Statistical Study of Atmospheric Turbulence by Thorpe Analysis. Journal of Geophysical Research D: Atmospheres, 2019, 124, 2897-2908.	3.3	16
49	A numerical study on amplitude characteristics of the terdiurnal tide excited by nonlinear interaction between the diurnal and semidiurnal tides. Earth, Planets and Space, 2007, 59, 183-191.	2.5	15
50	A numerical study on nonresonant interactions of gravity waves in a compressible atmosphere. Journal of Geophysical Research, 2007, 112, .	3.3	15
51	Propagation and reflection of gravity waves in a meridionally sheared wind field. Journal of Geophysical Research, 2008, 113, .	3.3	15
52	Atmospheric waves and their interactions in the thermospheric neutral wind as observed by the Arecibo incoherent scatter radar. Journal of Geophysical Research, 2012, 117, .	3.3	15
53	The <i>F</i> region and topside ionosphere response to a strong geomagnetic storm at Arecibo. Journal of Geophysical Research: Space Physics, 2013, 118, 5177-5183.	2.4	15
54	Simultaneous upward and downward propagating inertiaâ€gravity waves in the MLT observed at Andes Lidar Observatory. Journal of Geophysical Research D: Atmospheres, 2017, 122, 2812-2830.	3.3	15

#	Article	IF	CITATIONS
55	Study of Mean Wind Variations and Gravity Wave Forcing Via a Meteor Radar Chain and Comparison with HWMâ€07 Results. Journal of Geophysical Research D: Atmospheres, 2018, 123, 9488-9501.	3.3	15
56	Observational evidence of quasi-27-day oscillation propagating from the lower atmosphere to the mesosphere over 20° N. Annales Geophysicae, 2015, 33, 1321-1330.	1.6	15
57	Some ubiquitous features of the mesospheric Fe and Na layer borders from simultaneous and commonâ€volume Fe and Na lidar observations. Journal of Geophysical Research, 2008, 113, .	3.3	14
58	A Statistical Study of Inertia Gravity Waves in the Lower Stratosphere Over the Arctic Region Based on Radiosonde Observations. Journal of Geophysical Research D: Atmospheres, 2018, 123, 4958-4976.	3.3	14
59	Study of the Quasi 10â€Ðay Waves in the MLT Region During the 2018 February SSW by a Meteor Radar Chain. Journal of Geophysical Research: Space Physics, 2021, 126, e2020JA028367.	2.4	14
60	Thirdâ€order resonant interaction of atmospheric gravity waves. Journal of Geophysical Research D: Atmospheres, 2013, 118, 2197-2206.	3.3	13
61	Climatology of global gravity wave activity and dissipation revealed by SABER/TIMED temperature observations. Science China Technological Sciences, 2014, 57, 998-1009.	4.0	13
62	MST Radars of Chinese Meridian Project: System Description and Atmospheric Wind Measurement. IEEE Transactions on Geoscience and Remote Sensing, 2016, 54, 4513-4523.	6.3	13
63	An incoherent scatter radar study of the midnight temperature maximum that occurred at Arecibo during a sudden stratospheric warming event in January 2010. Journal of Geophysical Research: Space Physics, 2016, 121, 5571-5578.	2.4	13
64	Climatology of the Quasiâ€6â€Ðay Wave in the Mesopause Region and Its Modulations on Total Electron Content During 2003–2017. Journal of Geophysical Research: Space Physics, 2019, 124, 573-583.	2.4	13
65	Study of a Quasi 4â€Đay Oscillation During the 2018/2019 SSW Over Mohe, China. Journal of Geophysical Research: Space Physics, 2020, 125, e2019JA027687.	2.4	13
66	Inertia-gravity wave energy and instability drive turbulence: evidence from a near-global high-resolution radiosonde dataset. Climate Dynamics, 2022, 58, 2927-2939.	3.8	13
67	Vertical wavenumber spectra of three-dimensional winds revealed by radiosonde observations at midlatitude. Annales Geophysicae, 2017, 35, 107-116.	1.6	12
68	Climatological characteristics of planetary boundary layer height over Japan. International Journal of Climatology, 2019, 39, 4015-4028.	3.5	12
69	Climatology and Anomaly of the Quasiâ€īwoâ€Day Wave Behaviors During 2003–2018 Austral Summer Periods. Journal of Geophysical Research: Space Physics, 2019, 124, 544-556.	2.4	12
70	A Case Study of the Daytime Intense Radar Backscatter and Strong Ionospheric Scintillation Related to the Lowâ€Latitude Eâ€Region Irregularities. Journal of Geophysical Research: Space Physics, 2020, 125, e2019JA027532.	2.4	12
71	A numerical study on global propagations and amplitude growths of large-scale gravity wave packets. Journal of Geophysical Research, 2004, 109, .	3.3	11
72	A numerical study of the impact of nonlinearity on the amplitude of the migrating diurnal tide. Journal of Atmospheric and Solar-Terrestrial Physics, 2007, 69, 631-648.	1.6	11

#	Article	IF	CITATIONS
73	Observations of gravity wave activity during stratospheric sudden warmings in the Northern Hemisphere. Science China Technological Sciences, 2015, 58, 951-960.	4.0	11
74	The design of a form-changing female fitting robot. Journal of Advanced Mechanical Design, Systems and Manufacturing, 2016, 10, JAMDSM0097-JAMDSM0097.	0.7	11
75	Planetary Wave Characteristics in the Lower Atmosphere Over Xianghe (117.00°E, 39.77°N), China, Revealed by the Beijing MST Radar and MERRA Data. Journal of Geophysical Research D: Atmospheres, 2017, 122, 9745-9758.	3.3	11
76	Frequency variations of gravity waves interacting with a time-varying tide. Annales Geophysicae, 2013, 31, 1731-1743.	1.6	10
77	Lowâ€frequency oscillations of the gravity wave energy density in the lower atmosphere at low latitudes revealed by U.S. radiosonde data. Journal of Geophysical Research D: Atmospheres, 2016, 121, 13,458.	3.3	10
78	Latitudinal and Seasonal Variations of Vertical Wave Number Spectra of Threeâ€Dimensional Winds Revealed by Radiosonde Observations. Journal of Geophysical Research D: Atmospheres, 2017, 122, 13,174.	3.3	10
79	Laboratory fabrication of monolithic interferometers for one and two-dimensional spatial heterodyne spectrometers. Optics Express, 2017, 25, 29121.	3.4	10
80	Statistical Study of the Midlatitude Mesospheric Vertical Winds Observed by the Wuhan and Beijing MST Radars in China. Journal of Geophysical Research D: Atmospheres, 2020, 125, e2020JD032776.	3.3	10
81	A numerical study on the impact of nonlinear interactions on the amplitude of the migrating semidiurnal tide. Annales Geophysicae, 2006, 24, 3241-3256.	1.6	9
82	Atmospheric gravity wave excitation through sum nonresonant interaction. Journal of Atmospheric and Solar-Terrestrial Physics, 2011, 73, 2429-2436.	1.6	9
83	Spectral energy transfer of atmospheric gravity waves through sum and difference nonlinear interactions. Annales Geophysicae, 2012, 30, 303-315.	1.6	9
84	Facile synthesis of gold–platinum dendritic nanostructures with enhanced electrocatalytic performance for the methanol oxidation reaction. RSC Advances, 2016, 6, 51569-51574.	3.6	9
85	A Statistical Study of Fâ€Region 3.2â€mâ€Scale Fieldâ€Aligned Irregularities Occurrence and Vertical Plasma Drift Over Hainan: Solar Activity, Season, and Magnetic Activity Dependences. Journal of Geophysical Research: Space Physics, 2021, 126, e2020JA028932.	2.4	9
86	Comparison of stratospheric evolution during the major sudden stratospheric warming events in 2018 and 2019. Earth and Planetary Physics, 2020, 4, 1-11.	1.1	9
87	Statistics of lower tropospheric inversions over the continental United States. Annales Geophysicae, 2011, 29, 401-410.	1.6	8
88	The Tropopause Inversion Layer Interaction With the Inertial Gravity Wave Activities and Its Latitudinal Variability. Journal of Geophysical Research D: Atmospheres, 2019, 124, 7512-7522.	3.3	8
89	Signature of a Quasi 30â€Ðay Oscillation at Midlatitude Based on Wind Observations From MST Radar and Meteor Radar. Journal of Geophysical Research D: Atmospheres, 2019, 124, 11266-11280.	3.3	8
90	The vertical wave number spectra of potential energy density in the stratosphere deduced from the COSMIC satellite observation. Quarterly Journal of the Royal Meteorological Society, 2019, 145, 318-336.	2.7	8

#	Article	IF	CITATIONS
91	Multi-Instrument Observations of the Atmospheric and Ionospheric Response to the 2013 Sudden Stratospheric Warming Over Eastern Asia Region. IEEE Transactions on Geoscience and Remote Sensing, 2020, 58, 1232-1243.	6.3	8
92	Investigation of dominant traveling 10-day wave components using long-term MERRA-2 database. Earth, Planets and Space, 2021, 73, .	2.5	8
93	Understanding the Excitation of Quasiâ€6â€Đay Waves in Both Hemispheres During the September 2019 Antarctic SSW. Journal of Geophysical Research D: Atmospheres, 2022, 127, .	3.3	8
94	Statistical Characteristics of the Low‣atitude Eâ€Region Irregularities Observed by the HCOPAR in South China. Journal of Geophysical Research: Space Physics, 2022, 127, .	2.4	8
95	Characteristics of the quasi-16-day wave in the mesosphere and lower thermosphere region as revealed by meteor radar, Aura satellite, and MERRA2 reanalysis data from 2008 to 2017. Earth and Planetary Physics, 2020, 4, 274-284.	1.1	7
96	Investigation on Spectral Characteristics of Gravity Waves in the MLT Using Lidar Observations at Andes. Journal of Geophysical Research: Space Physics, 2021, 126, e2020JA028918.	2.4	7
97	Strong Quarterdiurnal Tides in the Mesosphere and Lower Thermosphere During the 2019 Arctic Sudden Stratospheric Warming Over Mohe, China. Journal of Geophysical Research: Space Physics, 2021, 126, e2020JA029066.	2.4	7
98	First Observational Evidence for the Role of Polar Vortex Strength in Modulating the Activity of Planetary Waves in the MLT Region. Geophysical Research Letters, 2022, 49, .	4.0	7
99	A numerical study on the response of wave number spectra of atmospheric gravity waves to lower atmospheric forcing. Journal of Geophysical Research, 2008, 113, .	3.3	6
100	Radiosonde observations of high-latitude planetary waves in the lower atmosphere. Science China Earth Sciences, 2010, 53, 919-932.	5.2	6
101	Characteristics of mid-latitude planetary waves in the lower atmosphere derived from radiosonde data. Annales Geophysicae, 2012, 30, 1463-1477.	1.6	6
102	A quasi-27-day oscillation activity from the troposphere to the mesosphere and lower thermosphere at low latitudes. Earth, Planets and Space, 2021, 73, .	2.5	6
103	Variations of Kelvin waves around the TTL region during the stratospheric sudden warming events in the Northern Hemisphere winter. Annales Geophysicae, 2016, 34, 331-345.	1.6	5
104	A mechanism to explain the variations of tropopause and tropopause inversion layer in the Arctic region during a sudden stratospheric warming in 2009. Journal of Geophysical Research D: Atmospheres, 2016, 121, 11,932.	3.3	5
105	Opposite Latitudinal Dependence of the Premidnight and Postmidnight Oscillations in the Electron Density of Midlatitude <i>F</i> Layer. Journal of Geophysical Research: Space Physics, 2018, 123, 796-807.	2.4	5
106	Strong downdrafts preceding rapid tropopause ascent and their potential to identify cross-tropopause stratospheric intrusions. Annales Geophysicae, 2018, 36, 1403-1417.	1.6	5
107	Global characteristics of the westward-propagating quasi-16-day wave with zonal wavenumber 1 and the connection with the 2012/2013 SSW revealed by ERA-Interim. Earth, Planets and Space, 2021, 73, .	2.5	5
108	Climatology and seasonal variation of the thermospheric tides and their response to solar activities over Arecibo. Journal of Atmospheric and Solar-Terrestrial Physics, 2021, 215, 105592.	1.6	4

#	Article	IF	CITATIONS
109	Water vapor anomaly over the tropical western Pacific in El Niño winters from radiosonde and satellite observations and ERA5 reanalysis data. Atmospheric Chemistry and Physics, 2021, 21, 13553-13569.	4.9	4
110	A Climatology of Merged Daytime Planetary Boundary Layer Height Over China From Radiosonde Measurements. Journal of Geophysical Research D: Atmospheres, 2022, 127, .	3.3	4
111	High resolution full-spectrum water Raman lidar. Science China Technological Sciences, 2012, 55, 1224-1229.	4.0	3
112	High-resolution Beijing mesosphere–stratosphere–troposphere (MST) radar detection of tropopause structure and variability over Xianghe (39.75° N, 116.96° E), China. Annales Geophysicae, 2019, 37, 4	53 ¹⁻⁶ 43.	3
113	Anomalous changes of temperature and ozone QBOs in 2015â^'2017 from radiosonde observation and MERRA-2 reanalysis. Earth and Planetary Physics, 2021, 5, 1-10.	1.1	3
114	A Numerical Study of Gravity Waves Propagation Characteristics in the Mesospheric Doppler Duct. Journal of Geophysical Research D: Atmospheres, 2021, 126, e2021JD034680.	3.3	3
115	Wuhan MST radar: technical features and validation of wind observations. Atmospheric Measurement Techniques, 2020, 13, 5697-5713.	3.1	3
116	Modeling Studies of Gravity Wave Dynamics in Highly Structured Environments: Reflection, Trapping, Instability, Momentum Transport, Secondary Gravity Waves, and Induced Flow Responses. Journal of Geophysical Research D: Atmospheres, 2022, 127, .	3.3	3
117	A Numerical Study of Saturation Mechanisms of Gravity Waves in The Mesosphere. Chinese Journal of Geophysics, 2001, 44, 452-458.	0.2	2
118	Simulation of the equatorial quasi-biennial oscillation based on the parameterization of continuously spectral gravity waves. Science Bulletin, 2009, 54, 288-295.	9.0	2
119	Wave Mode Analyses of Gravity Waves Propagating in the Mesospheric Thermal Duct. Chinese Journal of Geophysics, 2010, 53, 42-53.	0.2	2
120	A Numerical Simulation on Gravity Waves Generated by Thermal Source and their Influences on Mean Flow. Chinese Journal of Geophysics, 2011, 54, 415-426.	0.2	2
121	A New Method for Measuring Atmospheric Temperature and Aerosol Backscattering Coefficient Using a Pure Rotational Raman Lidar. Chinese Journal of Geophysics, 2012, 55, 617-625.	0.2	2
122	A study on electric field mapping from the <i>F</i> region to the <i>E</i> region at Arecibo. Journal of Geophysical Research: Space Physics, 2016, 121, 713-718.	2.4	2
123	A Numerical Study of Gravity Wave Propagation Characteristics in the Stratospheric Thermal Duct. Journal of Geophysical Research D: Atmospheres, 2018, 123, 11,918.	3.3	2
124	Effect of Temperature and Vertical Drift on Helium Ion Concentration Over Arecibo During Solar Maximum. Journal of Geophysical Research: Space Physics, 2019, 124, 9194-9202.	2.4	2
125	Study of a Quasiâ€₽7â€Đay Wave in the MLT Region During Recurrent Geomagnetic Storms in Autumn 2018. Journal of Geophysical Research: Space Physics, 2021, 126, e2020JA028865.	2.4	2
126	Effect of Semidiurnal Lunar Tides Modulated by Quasiâ€2â€Day Wave on Equatorial Electrojet During Three Sudden Stratospheric Warming Events. Geophysical Research Letters, 2021, 48, e2021GL095352.	4.0	2

#	Article	IF	CITATIONS
127	Design of the New MST Radar in Chinese Meridian Project. IEEE Journal of Selected Topics in Applied Earth Observations and Remote Sensing, 2021, 14, 2689-2698.	4.9	2
128	Latitudinal- and height-dependent long-term climatology of propagating quasi-16-day waves in the troposphere and stratosphere. Earth, Planets and Space, 2021, 73, .	2.5	2
129	A Statistical Investigation of Inertia Gravity Wave Activity Based on MST Radar Observations at Xianghe (116.9°E, 39.8°N), China. Journal of Geophysical Research D: Atmospheres, 2022, 127, .	3.3	2
130	Observations of a Strong Intraseasonal Oscillation in the MLT Region During the 2015/2016 Winter Over Mohe, China. Journal of Geophysical Research: Space Physics, 2022, 127, .	2.4	2
131	A topographic parameter inversion method based on laser altimetry. Science China Technological Sciences, 2012, 55, 1273-1280.	4.0	1
132	A numerical study on matching relationships of gravity waves in nonlinear interactions. Science China Earth Sciences, 2013, 56, 1079-1090.	5.2	1
133	The effect of Doppler broadening on <i>D</i> region negative ion ratio measurements at Arecibo. Journal of Geophysical Research: Space Physics, 2017, 122, 5816-5824.	2.4	1
134	An Unusually Large Electron Temperature Increase Over Arecibo Associated With an Intense Geomagnetic Storm. Journal of Geophysical Research: Space Physics, 2021, 126, e2021JA029836.	2.4	1
135	Statistical spectral characteristics of threeâ€dimensional winds in the mesopause region revealed by the Andes lidar. Journal of Geophysical Research D: Atmospheres, 2021, 126, e2021JD035586.	3.3	1
136	The First Observation of Additional Ionospheric Layers Over Arecibo Using an Incoherent Scatter Radar. Geophysical Research Letters, 2022, 49, .	4.0	1
137	Longâ€term Study of Quasiâ€16â€day Waves Based on ERA5 Reanalysis Data and EOSÂMLS Observations From 2005 to 2020. Journal of Geophysical Research: Space Physics, 0, , .	2.4	1
138	Long-Term Observation of the Quasi-3-Hour Large-Scale Traveling Ionospheric Disturbances by the Oblique-Incidence Ionosonde Network in North China. Sensors, 2022, 22, 233.	3.8	1
139	Observations of eastward propagating quasi $6\hat{a}\in$ day waves from the troposphere to the lower thermosphere during SSWs in early 2016. Journal of Geophysical Research D: Atmospheres, 0, , .	3.3	1
140	Extraordinary quasi-16-day wave activity from October 2013 to January 2014 with radar observations at mid-latitudes and MERRA2 reanalysis data. Earth, Planets and Space, 2022, 74, .	2.5	1
141	A Numerical Simulation on Gravity Waves Propagation in Mesospheric Thermal Duct. Chinese Journal of Geophysics, 2007, 50, 891-901.	0.2	0
142	A Numerical Study on Gravity Wave Excited Through Nonresonant Interaction. Chinese Journal of Geophysics, 2007, 50, 28-40.	0.2	0
143	Traveling 10-Day Waves at Mid-Latitudes in the Troposphere and Lower Stratosphere Revealed by Radiosonde Observations and MERRA-2 Data in 2020. Atmosphere, 2022, 13, 656.	2.3	0